Certification-Informed Analytical Preliminary Structural Design of a Box-Beam Engine Pylon for a Representative Wide-Body Civil Aircraft

Ayush Kamboj
ORCID: 0009-0000-6351-8382
Cranfield University, Faculty of Engineering and Applied Sciences
Cranfield, Bedfordshire, United Kingdom
Email: mdkayushkamboj@gmail.com
Corresponding author

Abstract

Objectives: This study develops a certification-informed analytical framework for the preliminary structural design of an under-wing box-beam engine pylon representative of a twin-engine wide-body civil aircraft. The objective is to link airworthiness-derived loading requirements, engine–pylon reactions, structural architecture and geometry-based mass assessment within a traceable early-design workflow.

Methods: Three aircraft mass states, five characteristic speeds and nine altitude conditions define the baseline design space. Gust, gyroscopic, engine failure, engine seizure, and emergency loading are evaluated to establish six-component reaction envelopes. These loads are transferred through an idealised closed box-beam representation to derive internal shear-force, bending-moment and torsional distributions and to support preliminary structural sizing of skins, ribs, stiffeners, spar caps and attachment lugs.

Results: The final configuration contains 12 ribs and transitions from integral blade stiffeners in the central box to four L-section spar caps in geometrically constrained tapered regions. The CAD-based structural mass is approximately 596 kg per pylon, with the Ti-6Al-4V primary structure contributing approximately 85%.

Conclusions: The methodology provides a transparent analytical route from certification-informed loading to preliminary structural architecture and mass assessment. No finite-element stress, displacement or buckling results are used as validation evidence; higher-fidelity numerical and experimental verification remains necessary.

Keywords: Aircraft Structures; Engine Pylons; Structural Design; Load Analysis; Wide-Body Aircraft; Structural Sizing.

Introduction

Aircraft engine pylons form the primary mechanical interface between an externally mounted propulsion system and the airframe. They transmit thrust, inertia, lateral and vertical forces, torque and bending moments through discrete engine and wing attachments. Consequently, pylon loading is inherently three-dimensional and sensitive to attachment stiffness and load redistribution (Luo et al. 2014; Wang et al. 2025).

The design envelope extends beyond steady thrust and weight to manoeuvre- and gust-induced inertia, gyroscopic effects, engine torque, seizure or failure conditions and emergency landing loads. Integrated airframe-propulsion studies show that abnormal and flight loads can govern different structural responses, while simplified equivalent-static representations remain useful during early sizing (Quinn et al. 2025; Colbert et al. 2023).

A second challenge is selecting an analysis fidelity level appropriate to the design's maturity. Detailed finite-element models can resolve local deformation, attachment-load redistribution and joint behaviour, but they require sufficiently mature geometry, stiffness definitions, boundary conditions and connection modelling. During preliminary design, reduced-order analytical models remain valuable because they provide transparent load paths, rapid evaluation of alternative structural concepts and direct traceability between applied loads and structural sizing assumptions. Higher-fidelity numerical analysis is therefore treated in the present study as a subsequent verification activity rather than as a prerequisite for establishing the preliminary structural architecture (Colbert et al. 2020; Colbert et al. 2022). Early integration of certification-derived requirements can also improve traceability between engineering decisions and subsequent substantiation activities (Kamboj and Sun 2026a). Related work within the same conceptual-design programme has applied this early-stage philosophy to stabilator load-envelope assessment and certification-informed fuel-system architecture (Kamboj and Sun 2026b; 2026c).

Preliminary aircraft-structure research has demonstrated the value of physics-based models that can be generated from limited design information and progressively refined as structural definition matures (Dorbath et al. 2011; Dorbath 2014; Pan et al. 2026). Closed box-beam configurations are particularly relevant to engine pylons because they provide efficient load paths for combined bending, shear and torsion while permitting local reinforcement around attachment regions (Bol and Ramulu 2020).

Existing research provides substantial coverage of pylon testing, detailed numerical idealisation, propulsion system dynamics, and structural optimisation. Comparatively less attention is given to transparent preliminary design workflows that begin with certification-derived loading requirements and proceed through engine-reaction envelopes, internal structural resultants, component-level analytical sizing decisions, and geometry-based mass assessment using limited non-proprietary information. This study addresses that need through a representative wide-body under-wing pylon case study. Public aircraft and propulsion characteristics are used only as configuration benchmarks; no proprietary production pylon is reproduced.

The principal contribution is a traceable analytical workflow linking certification-informed load definition to structural architecture. The methodology establishes representative engine–pylon loading conditions, derives six-component reaction envelopes and internal pylon resultants, applies classical structural mechanics to the primary load-carrying components, identifies a packaging-driven transition from blade stiffeners to spar caps, and quantifies the resulting CAD-based structural mass. The study is intentionally restricted to a preliminary analytical design; finite-element stress, displacement, and buckling verification is reserved for subsequent model maturation.

Design Basis and Case-Study Definition

Representative Aircraft and Propulsion Configuration

The methodology is demonstrated using a representative twin-engine wide-body civil transport with under-wing high-bypass turbofan propulsion. Publicly available transport-aircraft data are used only to establish an early-design context, consistent with representative propulsion-integration modelling based on non-proprietary information (Colbert et al. 2020).

A GEnx-1B-67-class engine is used as the propulsion benchmark. Because detailed proprietary geometry was unavailable during preliminary geometric development, a comparable GE90-94B-class model was used only as an external packaging surrogate for preliminary installation envelopes and attachment locations.

Pylon Structural Configuration

A closed box-beam architecture was selected to provide a continuous load path between the engine and wing attachments for combined bending, shear and torsion. The configuration extends from the forward engine-support region through the wing front-spar attachment to an aft pylon attachment between the principal wing spars.

The representative envelope has a maximum width of 0.510 m and a maximum structural depth of 1.008 m. The internal structure comprises skins, ribs, longitudinal blade stiffeners, spar caps and discrete attachment fittings.

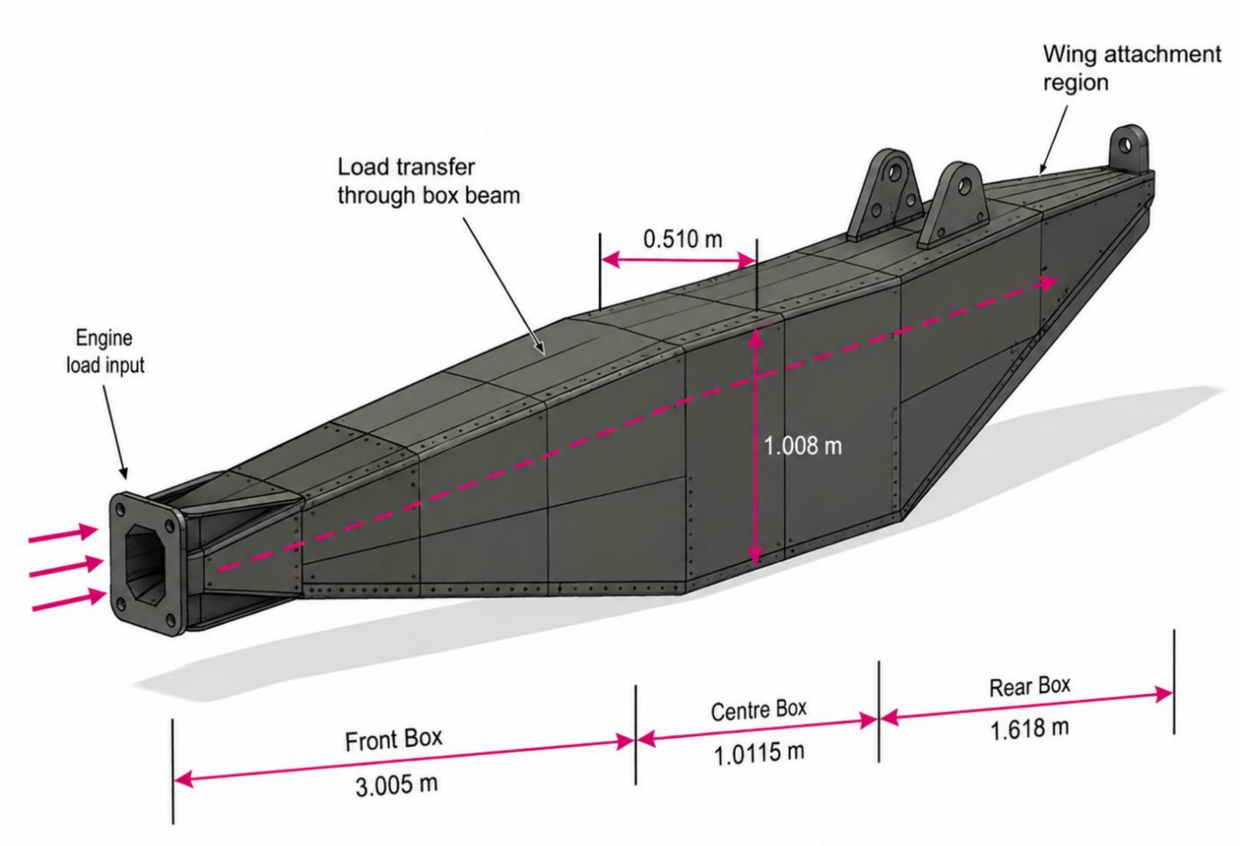

Figure 1. Representative external geometry and principal dimensions of the box-beam engine pylon.

Material Definition

A metallic baseline was retained for analytical tractability and thermal/structural robustness. Ti-6Al-4V was selected for the skins, ribs, stiffeners and spar caps, while S99 high-strength steel was assigned to the highly loaded attachment lugs. The selection reflects the specific considerations of strength, fatigue, temperature, and manufacturability typical of aerospace structural materials (Boyer et al. 2015).

Table 1. Baseline structural definition for the representative pylon.

Parameter	**Baseline definition**
Aircraft class	Twin-engine wide-body civil transport
Propulsion arrangement	Under-wing high-bypass turbofan
Propulsion reference	GEnx-1B-67-class
Geometric engine surrogate	GE90-94B-class external geometry
Pylon architecture	Closed box-beam

Parameter	Baseline definition
Maximum width	0.510 m
Maximum structural depth	1.008 m
Primary structural elements	Skins, ribs, stiffeners, spar caps
Primary structure material	Ti-6Al-4V
Attachment-lug material	S99 high-strength steel
Design stage	Preliminary structural design

Modelling Assumptions

The structural model is formulated at preliminary analytical fidelity. Engine thrust is assumed parallel to the aircraft longitudinal axis, and the engine–pylon assembly is treated as rigid during external-load generation. Table 2 summarises the principal modelling assumptions and exclusions.

Table 2. Principal analytical assumptions.

Assumption	Treatment in present study
Engine thrust direction	Parallel to aircraft longitudinal axis
Engine structural representation	Rigid body for preliminary load generation
Pylon self-weight	Neglected in initial external-load derivation
Nacelle aerodynamic lift	Neglected
Thermal expansion	Neglected
Contact and fastener load redistribution	Outside the present analytical fidelity
Detailed joint flexibility	Not explicitly modelled
Aeroelastic coupling	Reserved for higher-fidelity analysis
Bird-strike/empirical impact cases	Outside analytical scope
Structural analysis level	Preliminary analytical sizing and architecture definition

Accordingly, the analytical results reported in this study should be interpreted as global preliminary-design quantities. Local stress concentrations, attachment load sharing, structural deformation and buckling mode shapes are not directly resolved.

Preliminary Design-Space Definition

The operating design space combines three aircraft mass states (MTOM, ZFM and OEM), five characteristic speeds (V_{S1}, V_A, V_B, V_C and V_D) and nine altitudes from sea level to 13,000 m. These combinations define the baseline operating matrix used for the subsequent load cases.

CS-25 Structural Design Requirements

Regulatory Basis

The preliminary loading framework is informed by the European Union Aviation Safety Agency Certification Specifications for Large Aeroplanes (CS-25). Selected provisions are used to identify structurally relevant loading categories, distinguish limit and ultimate design actions, and establish traceability between regulatory requirements and the analytical load cases considered in this study. The use of these provisions is limited to preliminary design guidance and load-definition purposes and does not constitute demonstration of CS-25 compliance or certification substantiation.

For the applicable preliminary load cases considered here, the relationship between limit and ultimate design actions follows the 1.5 factor associated with the selected CS-25 strength provisions:

$$L_{ult} = 1.5\ L_{lim} \qquad (1)$$

where L_{lim} and L_{ult} denote the corresponding limit and ultimate force or moment quantities. Emergency-landing cases are treated separately because their loading basis is not represented simply by scaling the displayed limit envelope.

Pylon-Specific Loading Requirements

The principal EASA CS-25 provisions translated into the preliminary loading framework are summarised in Table 3.

Table 3. Selected CS-25 provisions used to inform the preliminary pylon loading framework.

CS-25 reference	Requirement relevant to pylon design	Treatment in present study	Structural implication
CS 25.303	Factor of safety	1.5 factor applied to applicable limit loads	Establishes ultimate sizing loads
CS 25.305	Strength and deformation	Provides context for subsequent structural-strength assessment	Basis for strength/reserve-factor evaluation
CS 25.341	Gust and turbulence loads	Representative gust-derived engine loading included	Vertical/lateral inertial load contribution
CS 25.361	Engine/APU torque	Engine torque considered within pylon loading	Introduces torsional demand in the pylon
CS 25.362	Engine failure loads	Representative failure case included; detailed transient dynamics excluded	Preliminary abnormal-load assessment only
CS 25.363	Side load	Lateral engine loading considered	Lateral bending, shear and mount loading
CS 25.371	Gyroscopic loads	Gyroscopic load case included analytically	Combined moments due to engine rotation and aircraft motion
CS 25.561	Emergency landing	Representative emergency load case included	Extreme inertial loading of engine/pylon system

Scope of Regulatory Application

The quantitative envelope retains five principal loading groups: gust, gyroscopic, engine failure, engine seizure and emergency loading. Transient dynamics, aeroelasticity, detailed attachment behaviour, impact response, fatigue, damage tolerance and experimental substantiation are outside the present analytical scope.

Accordingly, the term "certification-informed" used throughout this paper denotes the use of selected airworthiness requirements to guide preliminary load definition and structural decision-making; it does not indicate that the resulting pylon configuration has been certified or demonstrated to comply with CS-25.

Engine–Pylon Load Analysis

The load analysis converts the representative operating conditions into the six engine–pylon reaction components required for preliminary structural sizing. Five loading groups are retained in the present analytical framework: gust, gyroscopic, engine failure, engine seizure and emergency loading. The resulting reactions are expressed as three orthogonal forces and three moments and are subsequently transferred through the pylon geometry to establish preliminary internal shear, bending and torsional resultants.

Coordinate System and Rigid-Body Load Formulation

A body-fixed Cartesian system is used, with translational reactions F_x, F_y and F_z and moments M_x, M_y and M_z. This six-component representation is consistent with pylon interface-load descriptions used in experimental and numerical studies (Luo et al. 2014; Zettel et al. 2026).

For an arbitrary engine point P with position vector rP, the local rigid-body velocity and acceleration are represented by Eqs. (2) and (3).

$$v_P = V + \omega \times r_P \tag{2}$$

and

$$a_P = \dot{V} + \dot{\omega} \times r_P + \omega \times (\omega \times r_P) \tag{3}$$

where

$V = [U, V, W]^T$ and $\omega = [p, q, r]^T$ denote the aircraft translational and angular velocity vectors, respectively.

The corresponding translational inertia force at the engine centre of gravity is

$$F_I = -m_e \times a_{CG} \tag{4}$$

where m_e is the representative engine mass and aCG is its acceleration. Applied thrust, inertia and propulsion-induced moments are combined to obtain the reaction system transferred through the pylon.

Operating Design Matrix

The design matrix comprises three mass states, five characteristic speeds and nine altitude conditions, giving 135 baseline mass-speed-altitude combinations before the individual loading groups are applied.

Table 4. Preliminary load-analysis design space.

Variable	**Conditions considered**
Aircraft mass	MTOM, ZFM, OEM
Characteristic speeds	V_{S1}, V_A, V_B, V_C and V_D

Variable	Conditions considered
Altitudes	Sea level - 1500; 3000; 4500; 6000; 7500; 9000; 10500; 13000 m
Principal load groups	Gust, gyroscopic, engine failure, engine seizure, emergency
Output	F_x, F_y, F_z, M_x, M_y, M_z
Structural use	Preliminary Limit/ultimate envelope and internal pylon resultants

Principal Engine Loading Conditions

Gust loading is represented through the corresponding engine inertial reactions, while gyroscopic loading accounts for moments associated with changes in rotor angular momentum. Engine-failure and engine-seizure cases represent abnormal propulsion-system reactions and torque transfer, and emergency loading represents separately treated extreme inertial conditions. These cases are formulated as equivalent-static actions for preliminary structural sizing and do not reproduce the complete transient, vibration or aeroelastic response of the engine–pylon–airframe system (Colbert et al. 2023).

Limit and Ultimate Load Envelope

For each loading condition, the six reaction components were calculated and their positive and negative extrema collected. Applicable non-emergency ultimate loads were obtained with the 1.5 factor, whereas emergency-landing loading was treated separately. Table 5 therefore represents a component-wise reaction envelope rather than a single simultaneous six-component load vector.

The values in Table 5 are independently enveloped component extrema. An ultimate extreme need not equal 1.5 times the displayed limit extreme because different underlying cases may govern; the available record does not provide case-by-case identifiers.

Table 5. Independently enveloped limit and ultimate engine–pylon reaction extrema used for preliminary structural sizing.

Envelope	F_x (kN)	F_y (kN)	F_z (kN)	M_x (kN·m)	M_y (kN·m)	M_z (kN·m)
Limit maximum	306.5	51	170	974	1635	309
Limit minimum	95	−81	−170	−4.7	−902	−305

Ultimate maximum	460	181	362	1461	2453	463
Ultimate minimum	−543	−121	−255	−7	−1353	−457

Note: Component extrema are independently enveloped and do not represent a simultaneous six-component loading condition.

Internal Pylon Load Resultants

The independently derived external reaction cases were transferred through the representative pylon geometry to determine spanwise internal-load resultants. The resulting distributions comprise vertical shear force and bending moment, lateral shear force and bending moment, and axial torque, as shown in Figs. 2a–4. These quantities represent global analytical section resultants and should not be interpreted as local stress or deformation fields.

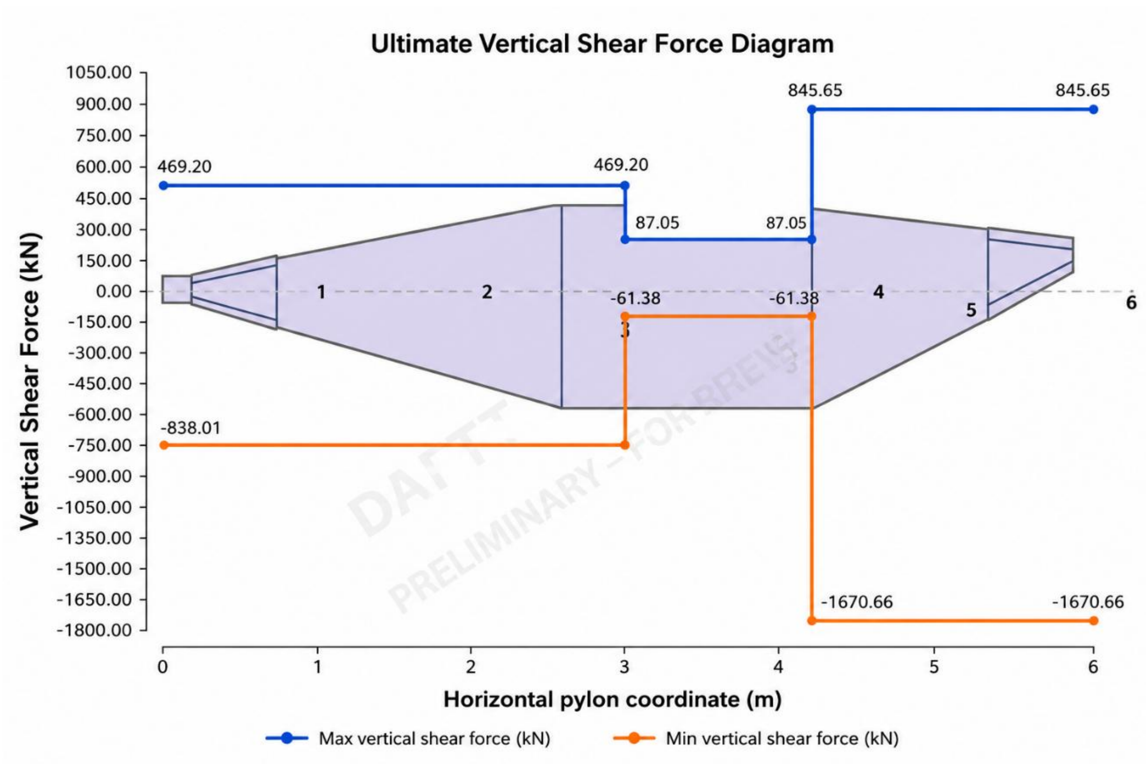

Figure 2a. Ultimate vertical internal-load distribution along the pylon: shear force.

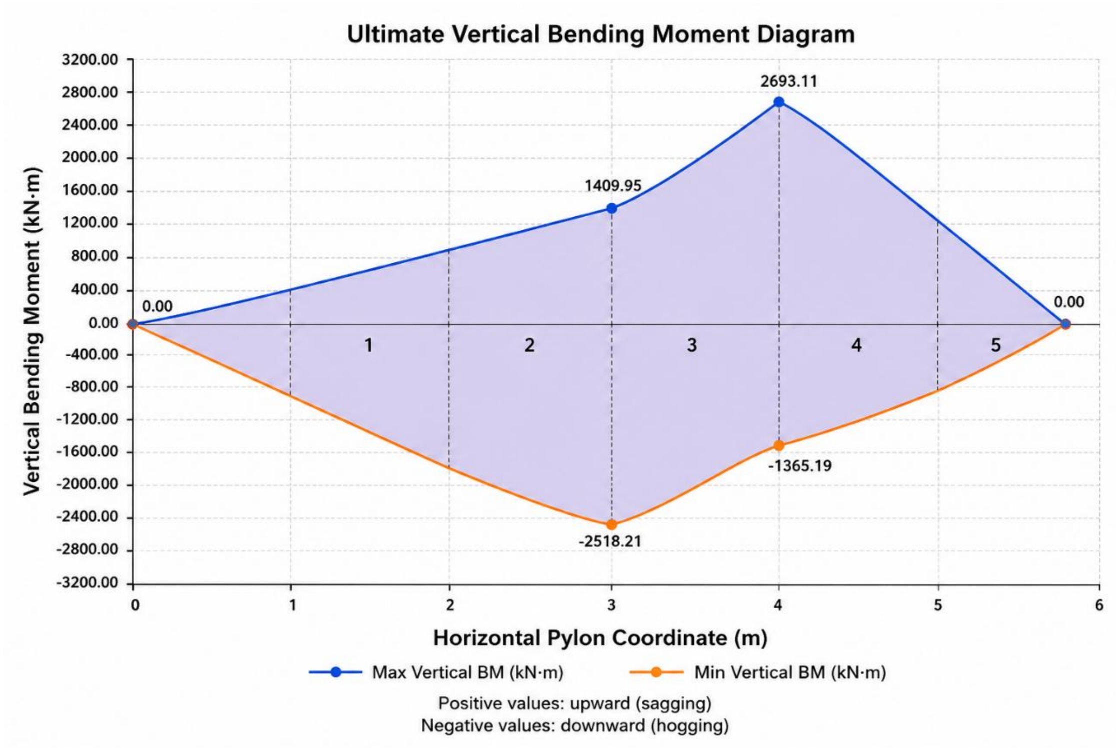

Figure 2b. Ultimate vertical internal-load distribution along the pylon: bending moment.

The vertical and lateral diagrams show strong changes across the attachment regions, while bending develops its largest magnitudes within the deeper central box.

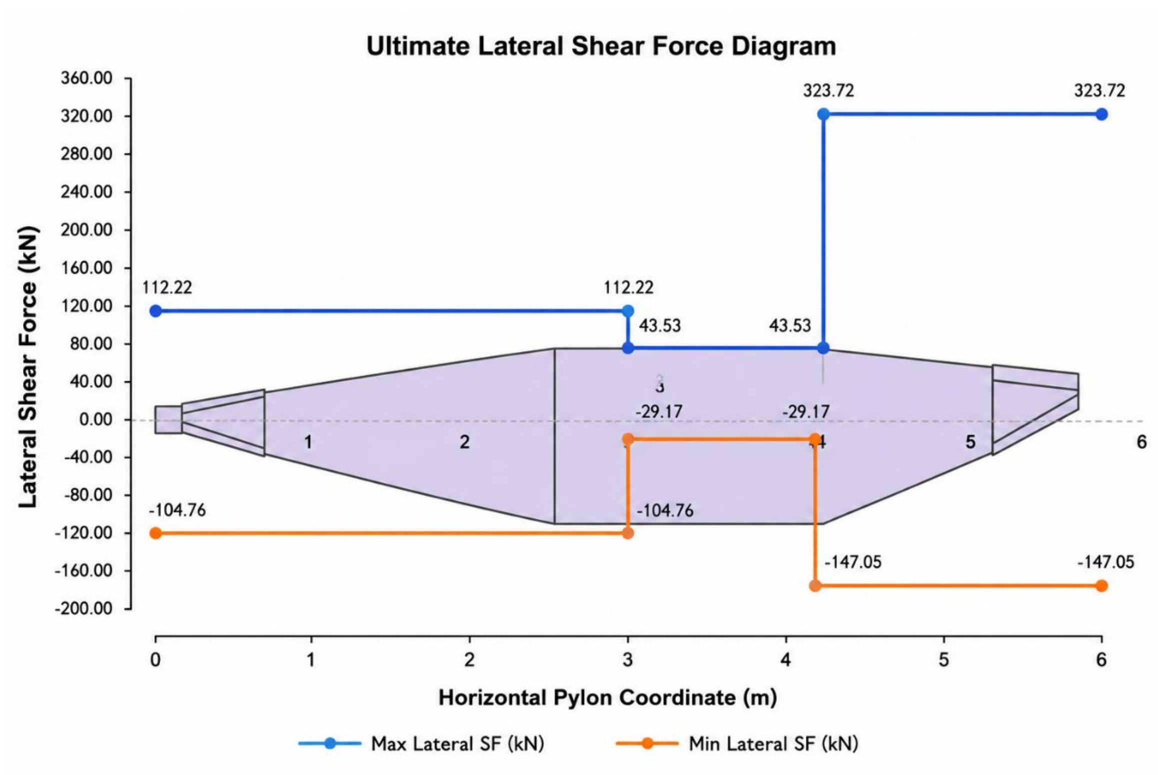

Figure 3a. Ultimate lateral internal-load distribution along the pylon: shear force.

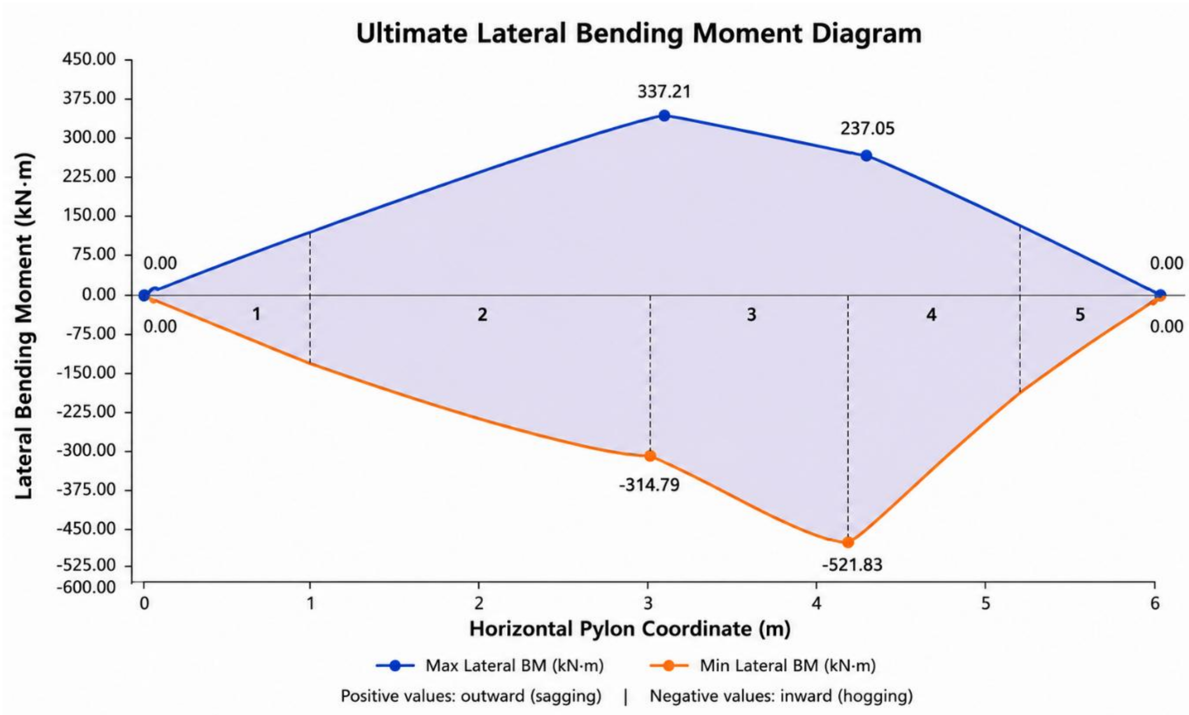

Figure 3b. Ultimate lateral internal-load distribution along the pylon: bending moment.

The torque distribution is also non-uniform because torque is introduced through discrete attachment locations and redistributed through the closed section before reaching the wing interface.

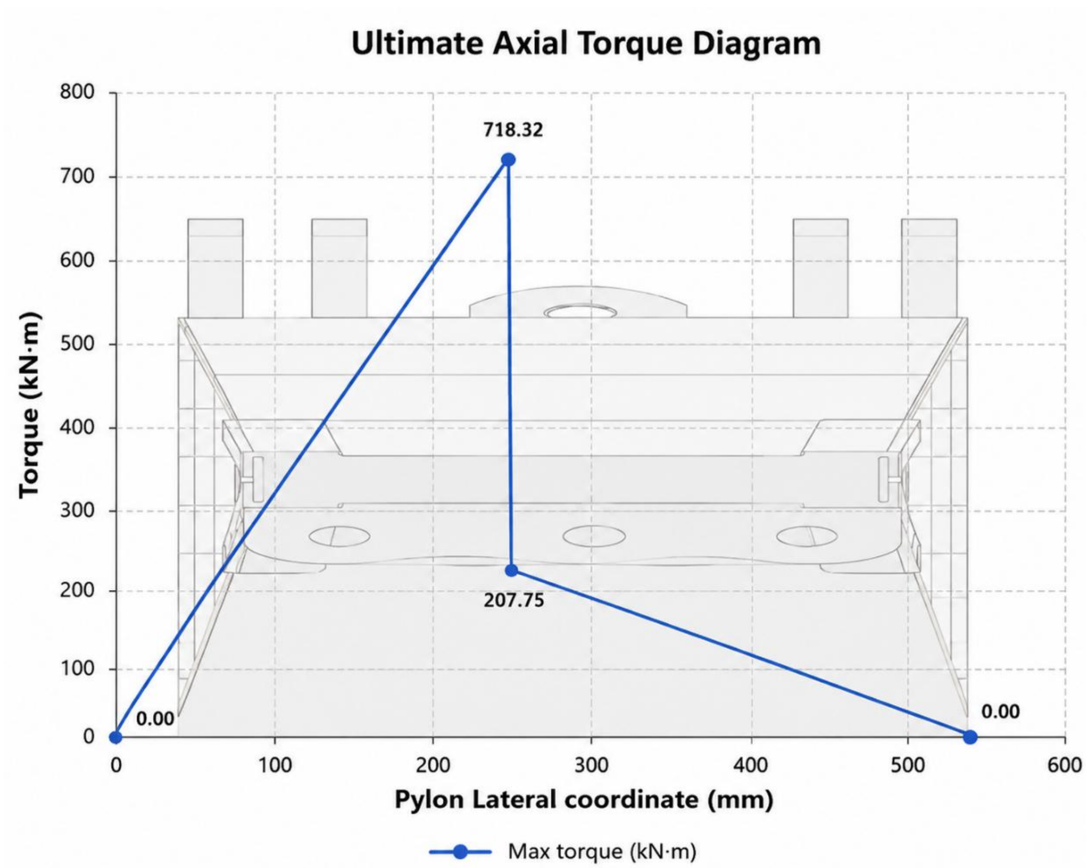

Figure 4. Ultimate axial torque distribution across the representative pylon section.

The analytical envelope demonstrates that preliminary pylon sizing cannot be based solely on thrust. Significant axial, vertical and lateral reactions occur together with bending and torsional demands, supporting the use of a closed-section structural concept. The reported distributions represent global preliminary load resultants rather than local structural responses. They do not resolve attachment flexibility, local stress concentrations, structural deformation, vibration, transient engine dynamics or aeroelastic coupling. Accordingly, they are used here to guide structural architecture and analytical sizing rather than to demonstrate detailed structural adequacy or certification compliance.

Box-Beam Pylon Structural Architecture

The preliminary load envelope was used to define a closed box-beam structural architecture intended to provide continuous load paths for axial force, transverse shear, bending and torsion between the engine and wing attachment regions. Closed box sections are well suited to preliminary pylon design because the skins, transverse ribs and longitudinal members can collectively resist multi-axis loading while maintaining a compact structural envelope (Niu 1989; Bol and Ramulu 2020). The configuration developed here should be interpreted as an analytically derived preliminary architecture rather than a structurally validated final design.

Structural Load Path

The representative pylon consists of tapered forward and aft regions connected through a deeper central box. Within the preliminary structural idealisation, engine reactions are introduced at the engine attachment regions and transmitted through reinforced ribs into the closed-section skins and longitudinal members before being transferred toward the wing attachment regions. This load path represents the intended global structural behaviour; detailed redistribution between individual fasteners, fittings, lugs and adjoining structural members is not resolved in the present analytical model.

The skins contribute to closed-section shear transfer and longitudinal bending resistance, the ribs preserve cross-sectional geometry and distribute concentrated interface actions, the longitudinal stiffeners provide additional compression and bending resistance in the central region, and the spar caps provide concentrated longitudinal load-carrying area where conventional blade stiffeners cannot be accommodated. Table 6 summarises these preliminary structural functions.

Table 6. Preliminary load-carrying functions of the principal pylon structural elements.

Structural element	Principal function in preliminary model	Principal analytical demand
Skins	Close box section and participate in load transfer	Shear, tension/compression, bending
Ribs	Maintain section shape and redistribute concentrated loads	Shear, local tension/compression
Stiffeners	Stabilise skins and provide longitudinal reinforcement	Compression/bending
Spar caps	Carry longitudinal loads where stiffeners cannot be accommodated	Bending-induced axial load
Attachment lugs	Introduce and transfer concentrated engine/wing loads	Tension, shear, bearing

The densities used for the CAD-based mass calculation were 4420 kg/m³ for Ti-6Al-4V and 7860 kg/m³ for S99 steel.

Rib Arrangement

Twelve ribs are distributed along the representative pylon, with locally reinforced rib regions associated with major attachment locations. Within the preliminary structural concept, the ribs preserve the box geometry and provide paths for redistribution of concentrated interface loads into the surrounding skins and longitudinal members. The number and spacing of ribs reflect the present case-study configuration and are not claimed to represent an optimised arrangement.

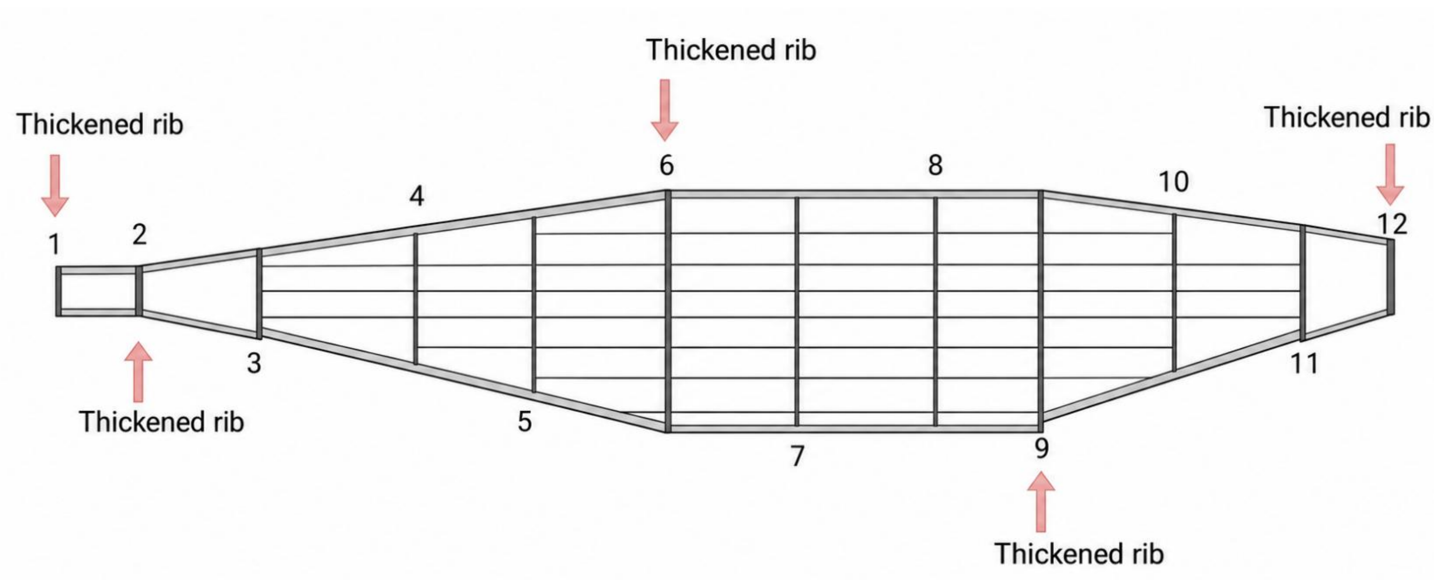

Figure 5. Internal structural arrangement showing the twelve rib stations and locally reinforced attachment regions.

Skin–Stiffener Arrangement

The deeper central box incorporates integral Ti-6Al-4V blade stiffeners as longitudinal reinforcement. Their intended functions are to increase the effective longitudinal stiffness of the skin panels and improve resistance to compression and bending-induced axial loading.

During preliminary sizing, required stiffener depths approached approximately 162 mm in regions where the available local box depth reduced to approximately 100 mm. The resulting geometric incompatibility, together with potential overlap between stiffeners on adjacent panels, made continuation of the blade-stiffener arrangement into the tapered regions impractical. The structural concept was therefore modified locally rather than imposing a uniform stiffener architecture along the full pylon length.

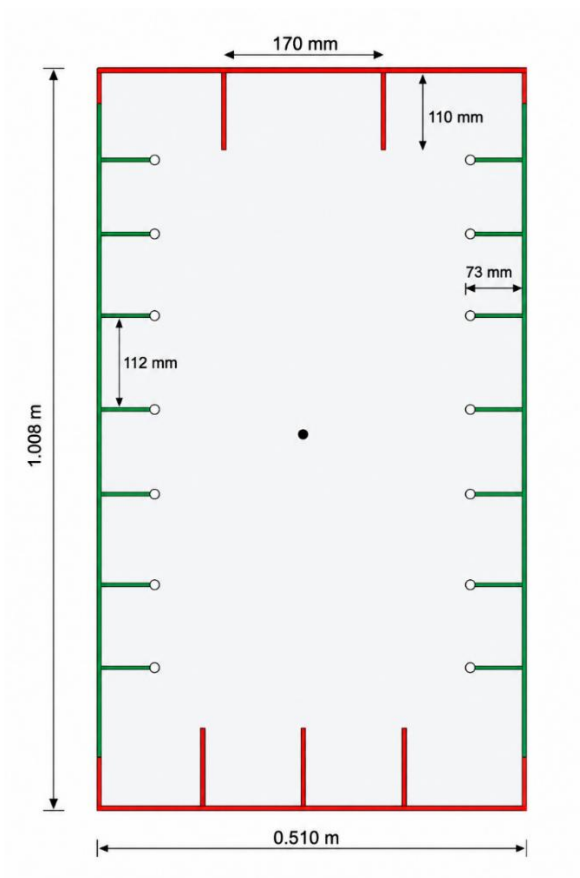

Figure 6. Arrangement of integral blade stiffeners within the central box region.

The architecture was therefore changed locally rather than forcing a uniform stiffener concept.

Spar-Cap Transition Regions

In the tapered forward and aft regions, four L-section spar caps—one located near each corner of the closed box—replace the blade-stiffener concept. In the representative configuration, spar-cap reinforcement extends approximately over Ribs 1–3 in the forward region and Ribs 11–12 in the aft region, while the central blade-stiffened region extends approximately between Ribs 3 and 11. This architectural transition was driven principally by geometric packaging constraints while preserving longitudinal load-carrying area near the corners of the closed section. The transition is therefore presented as a preliminary design solution rather than an optimised or numerically validated structural arrangement.

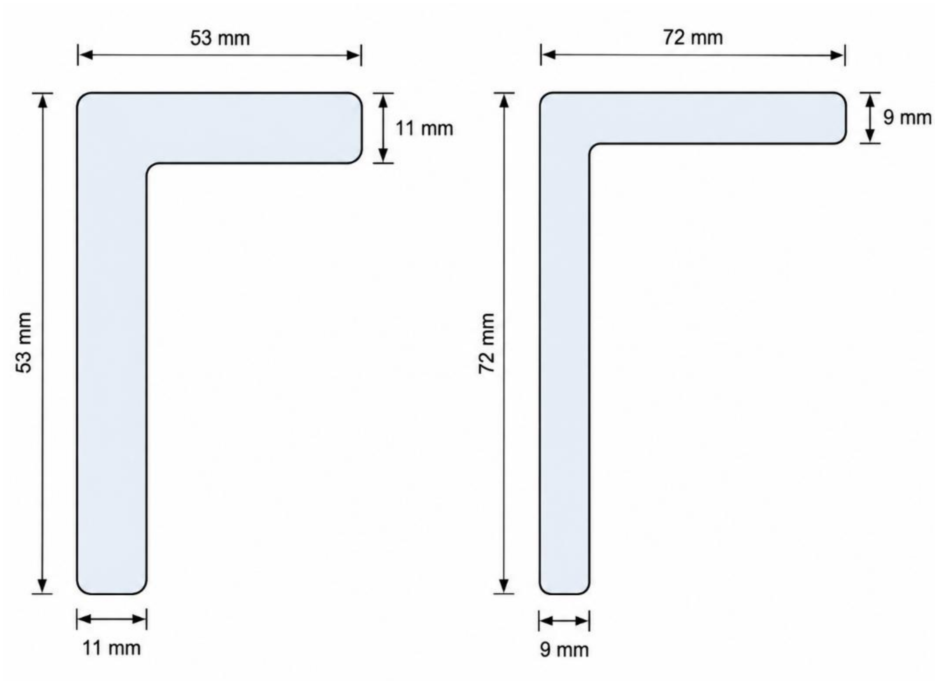

Figure 7. Representative L-section spar-cap geometries adopted in the tapered forward and aft regions.

The transition is governed by both structural demand and packaging feasibility.

Attachment Lugs

S99 steel attachment lugs represent the concentrated engine–pylon and pylon–wing load-introduction interfaces in the preliminary structural model. Their static analytical assessment is restricted to simplified net-section tension, pin bearing and shear-out checks. Local contact stresses, pin flexibility, fastener interactions, joint stiffness, three-dimensional stress concentrations, and load sharing among multiple attachments are unresolved. Fatigue and crack-growth substantiations are also outside the reproducible scope of the available dataset and are therefore not claimed in the present study.

Analytical Structural Sizing Methodology

The internal shear, bending and torsional resultants are treated as preliminary design actions for an idealised thin-walled, stiffened closed-section representation of the pylon. Classical aircraft structural mechanics are used to define the sizing criteria for skins, ribs, blade stiffeners, spar caps and attachment lugs (Niu 1989; Howe 2004; Megson 2021). The relations presented below establish the analytical basis for developing the structural configuration; they are not intended as a substitute for detailed finite-element stress analysis, joint modelling, or certification substantiation.

Analytical Strength Criterion

Where sufficient material and component data are available, a conventional reserve-factor formulation can be used to relate an allowable quantity to the corresponding analytical demand:

$$RF = \frac{Allowable\ structural\ capacity}{Applied\ structural\ demand} \quad (5)$$

For each failure mode, the relevant allowable stress or load is divided by the applied demand; the minimum value is governing.

Sectional Stress Evaluation

Combined axial and biaxial bending produce the normal stress

$$\sigma_x = \frac{N}{A} - \frac{M_y z}{I_y} + \frac{M_z y}{I_z} \quad (6)$$

where N is axial force, A is effective area, My and Mz are bending moments, Iy and Iz are the corresponding second moments of area, and y and z locate the evaluated point relative to the centroid.

For a thin-walled panel, transverse shear flow is

$$q_V = \frac{VQ}{I} \quad (7)$$

with panel shear stress obtained from τV = qV/t.

Here Q is the first moment of area, I the relevant second moment of area and t the local panel thickness.

For a single closed cell, the torsional shear flow is

$$q_T = \frac{T}{2A_m} \quad (8)$$

where T is torque and A_m is the area enclosed by the median line; the corresponding torsional shear stress is τT = qT/t.

Transverse and torsional shear contributions are combined with the appropriate sign for the panel location.

A preliminary combined-stress check uses the von Mises equivalent stress

$$\sigma_{\mathrm{vm}} = \sqrt{\sigma_x^2 + 3\tau^2} \tag{9}$$

which is compared with the applicable material allowable.

Skin Sizing

Skin thickness is governed by the most restrictive applicable direct-stress or stability requirement. Compression and shear buckling are represented using classical isotropic plate relations.

The elastic compressive buckling stress is

$$\sigma_{\mathrm{cr}} = k_c \frac{\pi^2 E}{12(1-\nu^2)} \left(\frac{t}{b}\right)^2 \tag{10}$$

where b is unsupported panel width and kc the corresponding buckling coefficient.

The elastic shear-buckling stress is

$$\tau_{\mathrm{cr}} = k_s \frac{\pi^2 E}{12(1-\nu^2)} \left(\frac{t}{b}\right)^2 \tag{11}$$

where ks is the shear-buckling coefficient.

Integral Blade-Stiffener Sizing

Blade stiffeners in the central box contribute to compression and bending resistance. Column stability is screened using Euler buckling; the stiffener arrangement is retained only where the required depth is compatible with the available box geometry.

For an effective unsupported length Le and end-restraint factor K,

$$P_{\mathrm{cr}} = \frac{\pi^2 E I_s}{(K L_e)^2} \tag{12}$$

where Is is the stiffener second moment of area.

Spar-Cap Sizing

Four L-section spar caps are used in the tapered regions. For a simplified bending couple with effective structural depth h, the total longitudinal force is approximated by

$$F_c = \frac{M}{h} \tag{13}$$

If two caps share the longitudinal force on one side of the section, each carries approximately half of this value. Combined vertical and lateral bending is assessed using the sectional stress relation in Eq. (6).

Rib Sizing

The 12 ribs maintain section geometry and redistribute panel shear and concentrated attachment loads. Mount-associated ribs are treated separately because of their higher local demand.

Attachment-Lug Sizing

Attachment lugs are assessed against net-section tension, pin bearing and shear-out.

For lug thickness tl, width w, hole diameter d and applied load P, the net-section stress is

$$\sigma_{\text{net}} = \frac{P}{t_l(w-d)} \tag{14}$$

The bearing stress is

$$\sigma_{\text{br}} = \frac{P}{t_l d} \tag{15}$$

Using the clear shear ligament C shown in Fig. 8, the simplified shear-out stress is

$$\tau_{\text{so}} = \frac{P}{2t_l e} \tag{16}$$

Analytical Sizing Workflow

The analytical workflow therefore progresses from certification-informed load definition to engine–pylon reaction envelopes, global internal-section resultants, component-level strength and stability criteria, structural architecture selection, and CAD-based mass assessment. The equations define the mechanics used to guide preliminary sizing and architecture development. Where the underlying component calculation records are incomplete, the present paper does not reconstruct or infer unsupported stress margins; such quantities are explicitly identified as requiring subsequent verification.

Results

The analytical workflow produced the global internal-load extrema, the selected preliminary structural architecture, principal geometric outputs and a CAD-based structural mass estimate. The results reported in this section are restricted to quantities that can be traced to the retained analytical calculations and geometric model. No finite-element stress, displacement or buckling results are presented as validation evidence.

Principal Internal-Load Extrema

The vertical envelope reaches 845.65 and −1670.66 kN in shear and 2693.11 and −2518.21 kN·m in bending; the lateral envelope reaches 323.72 and −147.05 kN in shear and 337.21 and −521.83 kN·m in bending.

The maximum reported axial torque is approximately 718.32 kN·m. These component extrema support the need for a closed section capable of combined bending, shear and torsion.

Selected Preliminary Structural Configuration

The final architecture is a closed metallic box with 12 ribs, central blade stiffeners, four L-section spar caps in the tapered regions and discrete attachment fittings.

The geometry-driven transition occurs because approximately 162 mm stiffeners could not be accommodated where local box depth reduced to about 100 mm.

The forward spar-cap section is 52.84 × 52.84 × 11 mm, and the aft section is 71.81 × 71.81 × 9 mm; Ti-6Al-4V is used for the primary structure and S99 steel for the attachment components.

Attachment-Lug Geometry

The representative S99 attachment lug has an overall width of approximately 180 mm, thickness of 70 mm and hole diameter of 40 mm. The geometry is used here only for static tension, bearing and shear assessment.

A subsequent fatigue/crack-growth assessment is documented, but its underlying inputs and outputs are unavailable; no independent damage-tolerance claim is therefore made.

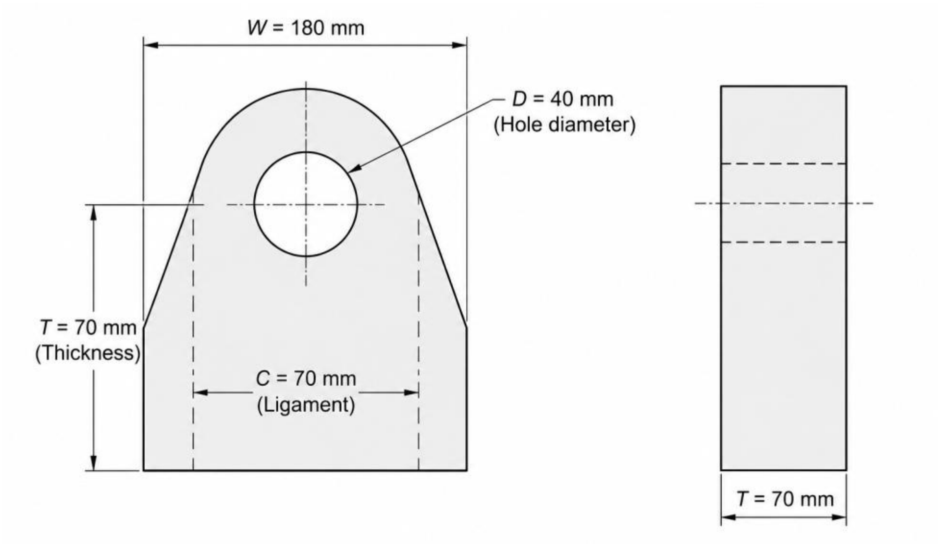

Figure 8. Geometric definition of the representative S99 attachment lug used for preliminary static tension, bearing and shear assessment.

Structural Sizing Outcome

Component reserve factors are not reported because the supporting stress and allowable worksheets are unavailable for independent reproduction.

Mass Assessment

The CAD-based structural mass is approximately 596 kg per pylon (Table 7), with the Ti-6Al-4V primary structure contributing approximately 85%. The fittings-and-fasteners contribution is estimated rather than explicitly modelled; the total therefore represents a preliminary structural mass rather than a complete production installation mass.

Table 7. Component-level mass breakdown of the preliminary engine pylon.

Component	Material	Density (kg/m³)	Volume (m³)	Mass (kg)	Total mass (%)
Pylon main structure	Ti-6Al-4V	4420	0.114	503	84.5
Wing-attachment lugs	S99 steel	7860	0.009	68	11
Engine-attachment lugs	S99 steel	7860	0.001	9.9	1.7
Fittings and fasteners	As required	—	—	14.5	2.4
Total	—	—	0.124	596	100

Displayed CAD volumes are rounded; component masses were calculated from the underlying geometric model. The primary box dominates mass and is therefore the principal target for future refinement.

Discussion

Structural implications of the load path

The results confirm that preliminary pylon design must address combined bending, shear and torsion rather than engine thrust alone. The closed box provides a direct load path between the engine and wing attachments, while concentrated reactions are redistributed through reinforced ribs, skins and longitudinal members.

The transition from integral blade stiffeners to spar caps is governed by both geometry and structural demand: a theoretically adequate member is not viable if it cannot be packaged within the available envelope. This interaction between sizing and architectural feasibility is consistent with the progressive-fidelity philosophy used in preliminary aircraft structural design (Pan et al. 2026).

Attachment and mass implications

Attachment regions remain important local design drivers because concentrated loads pass through comparatively small interfaces. The wing-attachment lugs account for more than 11% of the pylon mass, so joint stiffness, contact, and load sharing may influence both local stresses and subsequent mass refinement.

Because the Ti-6Al-4V primary box accounts for approximately 85% of the total mass, future weight reduction should focus mainly on distributed skins, ribs, stiffeners and spar caps. Formal pylon optimisation has not been performed here; topology and multilevel optimisation approaches provide logical future extensions once a verified baseline model is available (Remouchamps et al. 2011).

Role within preliminary aircraft design

The methodology occupies an intermediate level between empirical conceptual mass estimation and detailed finite-element substantiation. Its value is traceability from certification-informed loading to internal resultants, structural architecture and geometry-based mass using limited early-design information.

Higher-fidelity analysis becomes necessary when individual mount loads, local joint stresses, deformation, dynamic response, fatigue or damage tolerance become design-driving quantities.

Limitations and Future Work

The study is limited to preliminary analytical structural design. The load-generation model treats the engine-pylon assembly as rigid and neglects pylon flexibility, nacelle lift, self-weight, thermal deformation, detailed joint behaviour, vibration and aeroelastic coupling. Abnormal propulsion conditions are represented by equivalent loads and do not reproduce the complete transient engine-airframe response.

The analytical closed box captures global bending, shear and torsional load paths but not local stress concentrations or attachment load sharing.

Future work should develop a corrected shell-and-beam finite-element model, demonstrate mesh convergence and correlate numerical and analytical internal loads. Subsequent refinement should include explicit attachment modelling, transient failure/seizure response, engine vibration, fatigue and damage tolerance; recent pylon-wing interface research highlights the importance of dynamic load transfer at this stage (Zettel et al. 2026). Structural optimisation and experimental subcomponent testing should follow a verified baseline.

Conclusions

This study established a certification-informed analytical methodology for preliminary structural definition of a representative under-wing box-beam engine pylon. The framework links regulatory loading conditions, engine reactions, internal bending/shear/torsion distributions, structural architecture and geometry-based mass assessment within a traceable early-design process.

The analysis shows that the pylon must transmit significant multi-axis actions. A closed Ti-6Al-4V box with 12 ribs uses integral blade stiffeners in the deeper central region and four L-section spar caps in tapered regions where approximately 162 mm stiffeners could not be accommodated within about 100 mm of local depth.

The CAD-based mass is 596 kg per pylon, with the primary Ti-6Al-4V structure contributing approximately 85%, identifying the distributed box as the main target for later mass refinement.

The configuration is a preliminary analytical baseline rather than a certification-ready design. Finite-element convergence, detailed attachment modelling, dynamic response, fatigue/damage tolerance and experimental correlation remain necessary.

References

Bol E, Ramulu M (2020) Repeatability of a topology optimized tapered box beam additively manufactured with electron beam melted Ti-6Al-4V. Proceedings of the ASME 2020 International Mechanical Engineering Congress and Exposition, IMECE2020-24352, V02AT02A049.

Boyer RR, Cotton JD, Mohaghegh M, Schafrik RE (2015) Materials considerations for aerospace applications. MRS Bull 40(12):1055-1066.

Colbert S, Quinn D, Nolan DC, Fox R, Haynes P, O'Doherty-Jennings J (2020) Toward structural modelling strategies for characterization of future airframe-propulsion system interactions. AIAA AVIATION 2020 Forum, AIAA 2020-2655. doi:10.2514/6.2020-2655.

Colbert S, Quinn D, Nolan DC, Gaskell J, Fox R (2022) A whole aircraft aeroelastic model for evaluation of propulsion system idealizations. AIAA AVIATION 2022 Forum, AIAA 2022-3956. doi:10.2514/6.2022-3956.

Colbert S, Quinn D, Nolan DC, Fox R, Gaskell J (2023) Impact of airframe-propulsion system modeling strategies on key structural performance metrics. J Aircr 60(2):281-292. doi:10.2514/1.C036820.

Dorbath F, Nagel B, Gollnick V (2011) A knowledge based approach for automated modelling of extended wing structures in preliminary aircraft design. Deutscher Luft- und Raumfahrtkongress (DLRK 2011), Bremen, Germany, 27-29 September.

Dorbath F (2014) A flexible wing modeling and physical mass estimation system for early aircraft design stages. Doctoral dissertation, Technische Universität Hamburg-Harburg, Hamburg.

Howe D (2004) Aircraft Loading and Structural Layout. Professional Engineering Publishing, London.

Kamboj A, Sun Y (2026a) Integrating computer-aided design and model-based systems engineering for early zonal hazard analysis: application to a supersonic aircraft fuel system. Aerospace 13(5):413. doi:10.3390/aerospace13050413.

Kamboj A, Sun Y (2026b) Flight load evaluation of an all-moving stabilator for a conceptual commercial supersonic transport aircraft. Aircraft Engineering and Aerospace Technology.

Kamboj A, Sun Y (2026c) Conceptual fuel-system architecture design for a low-boom supersonic transport aircraft. Paper presented at: 17th International Conference on Mechanical and Aerospace Engineering (ICMAE 2026); 15-18 July 2026; London, UK.

Luo D, Tang W, Xue C, Zhang P (2014) Static test rig development and application for an airliner's hyperstatic aero-engine pylon structure. J Meas Eng 2(3):145-153.

Megson THG (2021) Aircraft Structures for Engineering Students. 7th ed. Butterworth-Heinemann/Elsevier.

Niu MCY (1989) Airframe Structural Design: Practical Design Information and Data on Aircraft Structures. 2nd ed. Conmilit Press, Burbank, CA.

Pan Y, Alam M, Whidborne J, Westwood M (2026) Rapid preliminary aircraft wing sizing for metallic and composite structures to support data-driven multidisciplinary design optimisation frameworks. Aerosp Sci Technol 177:112250. doi:10.1016/j.ast.2026.112250.

Quinn D, Colbert S, Nolan DC, Fox R, Gaskell J (2025) Propulsion system integration on truss-braced aircraft: structural performance sensitivity to architectural design parameters. Aerosp Sci Technol 159:109987. doi:10.1016/j.ast.2025.109987.

Remouchamps A, Bruyneel M, Fleury C, Grihon S (2011) Application of a bi-level scheme including topology optimization to the design of an aircraft pylon. Struct Multidisc Optim 44(6):739-750. doi:10.1007/s00158-011-0682-3.

Wang D, Niu Y, Guo X (2025) Dynamic analysis of aircraft engine-pylon coupled system. J Phys Conf Ser 3145:012031. doi:10.1088/1742-6596/3145/1/012031.

Zettel SF, Böswald M, Dewald RD, Winter R (2026) Jet engine vibration model for estimating pylon-wing interface loads for realistic structural excitation. CEAS Aeronaut J 17:1381-1394. doi:10.1007/s13272-025-00931-1.